Reactivity of $C_2H_5^+$ with Benzene: Formation of Ethylbenzenium Ions and Implications for Titan's Ionospheric Chemistry†

Jan Žabka,‡ Miroslav Polášek,‡ Daniela Ascenzi,*,⊥ Paolo Tosi,⊥ Jana Roithová,§,∥ and Detlef Schröder∥

J. Heyrovský Institute of Physical Chemistry, V. Čermák Laboratory, Academy of Sciences of the Czech Republic, Dolejškova 3, 18223 Prague 8, Czech Republic, Department of Organic Chemistry, Faculty of Sciences, Charles University in Prague, Hlavova 8, 12083 Prague 2, Czech Republic, Institute of Organic Chemistry and Biochemistry, Academy of Sciences of the Czech Republic, Flemingovo nám. 2, 166 10 Prague 6, Czech Republic, and Department of Physics, University of Trento, Via Sommarive 14 38100 Povo, Trento, Italy

Received: May 29, 2009; Revised Manuscript Received: July 6, 2009

The reaction of ethyl cation with benzene has been investigated in a combined experimental and theoretical approach. Under single collision conditions, proton transfer affording protonated benzene concomitant with neutral ethene represents the major reaction channel. From pressure-dependent measurements, an absolute cross section of 7 ± 2 Å^2 at hyperthermal energies (about 1.0 eV in the center of mass frame) is derived for this channel, from which a phenomenological rate constant of about 2.9×10^{-10} cm^3 s^{-1} is estimated at low energies. The energy behavior of the cross section as well as several side reactions leading to C−C coupling imply that the reaction of $C_2H_5^+$ with C_6H_6 proceeds via a long-lived association product, presumably the covalently bound protonated ethylbenzene (ethylbenzenium ion). With regard to chemical processes in the atmosphere of Titan, present results imply that termolecular association of $C_2H_5^+$ with benzene to produce protonated ethylbenzene is very likely to occur. The condensation of alkyl cations with arenes thus provides an alternative route for the growth of larger hydrocarbon molecules.

Introduction

In 2005, the first results of the Cassini−Huygens mission have boosted research about the chemistry of Titan atmosphere. Specifically, surprisingly large amounts of medium-sized hydrocarbon ions have been discovered which have previously not been expected in these amounts.[1] Accordingly, there is increased interest in possible routes for the formation of medium-sized, most likely aromatic hydrocarbons (and also nitrogen-heterocycles) under the conditions of the Titan atmosphere (ca. 100 K, 1 bar surface pressure). Seminal work of Anicich[2,3] has indicated that most of these C_mH_n species are formed via cationic routes which initially lead to the corresponding cations $C_mH_n^+$, which then undergo proton transfer, electron transfer, or hydride abstraction to afford neutral C_mH_{n-1}, C_mH_n, and C_mH_{n+1}, respectively. In the context of possible growth reactions of aromatic hydrocarbons in the higher atmosphere of Titan, recently the association of alkyl cations with neutral arenes has been also suggested.[4] Specifically, the ion chemistry of methane, the second most abundant component of Titan's atmosphere after nitrogen, is well-known to generate $C_2H_5^+$ as well as $C_3H_5^+$ cations.[5] Combined with the fact that carbenium ions such as $C_2H_5^+$ can electrophilically attack arenes,[6] it thus evolves the question if the reactions of small hydrocarbon cations with preformed, neutral arenes could provide a feasible route for the formation of larger $C_mH_n^+$ cations under the conditions of an extraterrestrial atmosphere.

To explore this question, we decided to investigate the reaction of $C_2H_5^+$ with benzene as a model for the scope and the relevance of this and similar processes in this context.[7] Ion/molecule reactions of benzene and substituted benzene reagents as well as their microscopic counterpart, the dissociation of protonated alkylbenzenes, have been investigated previously by a variety of techniques, ranging from the low-pressure regime[8–11] to a study of the high-pressure gas-phase chemistry of alkylbenzenium ions using radiolytic techniques.[6] Particularly noteworthy in this context is the detailed work of Kuck and coworkers on the gas-phase ion chemistry of ionized alkylbenzenes,[12] which is characterized by extensive and complicated intramolecular rearrangements including ring contractions and -expansion with subsequent carbon and H atom scrambling. Thus, ethylbenzenium ions are only one of the possible isomers of formula $C_8H_{11}^+$ (others being xylenium ions, protonated 6,6-dimethylfulvenes, methyltropylium ions, just to mention a few) and a variety of experimental and computational studies on the gas-phase chemistry of $C_8H_{11}^+$ ions have been performed[12–14] Recently, several theoretical papers dealt with the correct theoretical description of the addition of $C_2H_5^+$ to benzene.[15]

The ethyl cation is a common protonating agent in chemical ionization mass spectrometry. As $C_2H_5^+$ is a nonclassical carbocation having C_{2v} symmetry and a 3-center-2-electron bond,[16] transfer of a proton should in fact be facile because the ethylene molecule is already preformed. In particular $C_2H_5^+$ has a density of 50 cm^{-3} in the INMS spectrum measured during the T5 flyby on April 16, 2005 (averaged at about 1000 km altitude). According to the model of Vuitton et al. the calculated density at a similar altitude is 200 cm^{-3}.[7] The modeled density

† Part of the special section "Chemistry: Titan Atmosphere".

‡ J. Heyrovský Institute of Physical Chemistry, Academy of Sciences of the Czech Republic.

⊥ University of Trento.

§ Charles University in Prague.

∥ Institute of Organic Chemistry and Biochemistry, Academy of Sciences of the Czech Republic.

10.1021/jp905052h CCC: $40.75
Published on Web 07/30/2009

depends on the formation of the CH_5^+ ion in reactions 1 and 2 followed by proton transfer to ethene (reaction 3):

$$N_2H^+ + CH_4 \rightarrow CH_5^+ + N_2 \qquad k_1 = 8.9 \times 10^{-10}\ cm^3\ s^{-1} \quad (1)$$

$$CH_4^+ + CH_4 \rightarrow CH_5^+ + CH_3 \qquad k_2 = 1.1 \times 10^{-9}\ cm^3\ s^{-1} \quad (2)$$

$$CH_5^+ + C_2H_4 \rightarrow C_2H_5^+ + CH_4 \qquad k_3 = 1.5 \times 10^{-9}\ cm^3\ s^{-1} \quad (3)$$

Additionally, the ethyl cation is produced from the condensation reaction 4 of methyl cation CH_3^+ with a methane molecule, CH_3^+ being formed both via electro/photofragmentation of CH_4 and via reaction of the latter with N^+ to give CH_3^+ plus NH:[5]

$$CH_3^+ + CH_4 \rightarrow C_2H_5^+ + H_2 \qquad k_4 = 1.1 \times 10^{-9}\ cm^3\ s^{-1} \quad (4)$$

The modeled density of $C_2H_5^+$ is also influenced by depletion processes, and the modeling studies explicitly consider proton transfer to HCN (reaction 5), condensation with C_2H_4 (reaction 6), and dissociative electron recombination.

$$C_2H_5^+ + HCN \rightarrow HCNH^+ + C_2H_4 \qquad k_5 = 2.7 \times 10^{-9}\ cm^3\ s^{-1} \quad (5)$$

$$C_2H_5^+ + C_2H_4 \rightarrow C_3H_5^+ + CH_4 \qquad k_6 = 3.6 \times 10^{-10}\ cm^3\ s^{-1} \quad (6)$$

$$C_2H_5^+ + C_6H_6 \rightarrow C_6H_7^+ + C_2H_4 \qquad k_7 = 3.0 \times 10^{-9}\ cm^3\ s^{-1} \quad (7)$$

The model of Vuitton et al. overestimates the density of $C_2H_5^+$ by a factor 4, which might indicate that some sinks for $C_2H_5^+$ are missing in the model or some of the rate constants for the reactions in which $C_2H_5^+$ is involved are underestimated. The proton transfer from $C_2H_5^+$ to benzene (reaction 7) is included also in the model, but the rate constant $k_7 = 3.0 \times 10^{-9}$ cm^3 s^{-1} is a mere estimate, since no value was available in the literature. Here, we provide an absolute value for the proton-transfer reactive cross section σ at hyperthermal energies, from which a phenomenological rate constant is derived.

Experimental and Theoretical Methods

Experimental Methods. Most reactions were performed in a home-built guided-ion beam apparatus (GIB-MS), which consists of a tandem mass spectrometer with an OQOQ configuration (where O stands for octopole and Q stands for quadrupole).[17] Ions are generated by electron ionization (EI) of bromoethane with electrons having kinetic energies in the range of 70−100 eV. The first octopole O1 is operated as an ion guide, the quadrupole Q1 acts as a mass filter to select the parent ions $C_2H_5^+$ at m/z 29. The latter are injected into O2, which is surrounded by a collision cell filled with the desired neutral reactant, the pressure of which is monitored by a spinning rotor gauge (MKS SRG2). The kinetic energy of the projectile ion-beam, which determines the collision energy between the parent ions and rare gas molecules, can be varied from about 0 to 100 eV by changing the bias potential of O2. Product ions are mass analyzed by Q2 and detected by an electron multiplier. The ratio between the measured signal intensities of product and reactant ions is proportional to the effective integral cross section and its absolute value can be measured, in a beam-cell experiment, according to the Lambert−Beer law. For low pressures of neutral target (thin target limit) the Lambert−Beer law can be approximated as[18]

$$\frac{I_P}{I_0} = \sigma_P n l_{eff} \quad (8)$$

Here, I_P and I_0 are the intensity of products P and reagent ions, respectively (with $I_P \ll I_0$), n is the neutral gas density in the collision cell, and l_{eff} is the effective cell of the collision cell, equal to 12.0 ± 0.6 cm in our case. By measuring the slope of the plot of I_P/I_0 as a function of the neutral gas density (at sufficiently low densities to ensure single collision regime), we can obtain σ_P for each of the reaction channels. In such type of measurements, the accuracy is limited by uncertainties in the measurement of the gas pressure and by error propagation due to the calibration procedure necessary to establish the value of l_{eff}. We estimate that absolute cross section values are accurate within ± 30%.

The collision-induced dissociation (CID) mass spectra were measured on a ZAB2-SEQ tandem mass spectrometer with reverse double-focusing geometry (magnetic sector precedes electrostatic sector), equipped with a standard chemical ionization source with an operating pressure of ca. 1 mbar. The ion source conditions were as follows: emission current 0.5 mA; electron energy 70 eV; temperature, 150 °C. High-energy (8 keV) CID mass spectra of ions selected by the magnetic sector were obtained with helium as a collision gas, which was admitted in the second field-free region collision cell at pressure allowing 70% transmittance of the ion beam. Product ions were identified by their kinetic energy by scanning the electric sector thus affording mass-analyzed ion kinetic energy (MIKE) spectra.

A few additional experiments at enhanced mass resolution of the precursor and product ions were performed with a TSQ mass spectrometer having an EI source and a QOQ configuration as discussed elsewhere.[19]

Theoretical Methods. Structures and energies of protonated ethylbenzene, with emphasis on the mechanism for loss of an ethene molecule have been recently determined in several quantum chemical studies using different theoretical methods (i.e., B3LYP, MP2, SCS-MP2, CCSD, G3B3).[15] It was experimentally suggested that the fragmentation of protonated ethylbenzene (giving either ethene plus benzenium ion or benzene plus ethyl cation) proceeds via an ion−neutral complex.[6] However, simulations using B3LYP and MP2 methods gave conflicting results,[15d] showing that an adequate theoretical treatment was necessary for a correct prediction of the ion-neutral complex, and the failure of MP2 methods to locate the ethene/benzenium ion complex was due to basis set superposition errors affecting MP2.[15c] More recent theoretical treatments have tried to reconcile previous results using either extended versions of the MP2 method[15b] or the composite method Gaussian-3 G3B3.[15a]

On the basis of previous theoretical work, the calculations of relevant structures and energies for the main channels of the

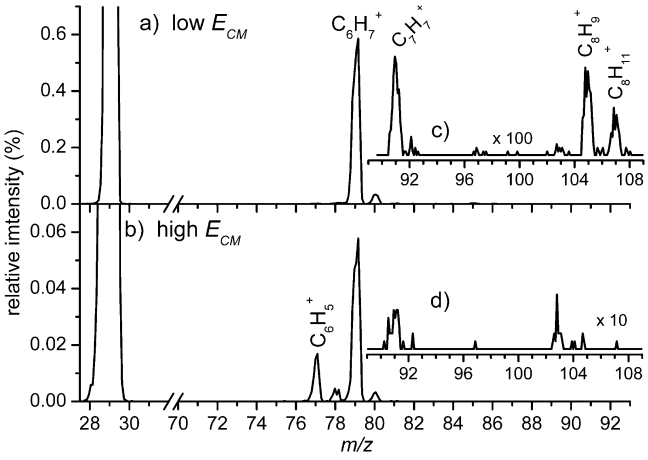

Figure 1. Reaction of mass-selected $C_2H_5^+$ ions with C_6H_6 at a benzene pressure of ca. 2.2×10^{-5} mbar in the reaction cell and at two different collision energies in the center-of-mass frame: (a) $E_{CM} = 1.3$ eV and (b) $E_{CM} = 4.5$ eV. The signal intensities of the parent ion (100.0) are off-scale. (c) and (d) show selected mass regions with the stated amplification factors.

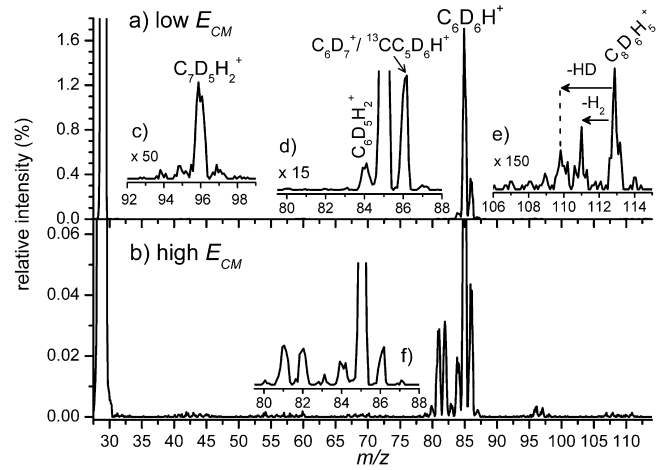

Figure 2. Reaction of mass-selected $C_2H_5^+$ ions with C_6D_6 at $p(C_6D_6) = 4.5 \times 10^{-5}$ mbar at nominal collision energies of $E_{CM} = 0.9$ eV for (a), (c)−(e) and $E_{CM} = 5.0$ eV for (b) and (f). The signal intensities of the parent ion (100.0) are off-scale. The insets (with given amplification factors) show the regions of the methane-loss products (c), the ethylene and ethane losses (d, f), and the $C_8H_5D_6^+$ product with hydrogen losses (e) at a C_6D_6 pressure of ca. 10^{-4} mbar and increased Q2 resolution.

reaction between $C_2H_5^+$ and benzene were performed in two steps using the Gaussian03 suite of programs.[20] In the first step, we employed standard density functional theory (DFT) for geometry optimization using Becke's hybrid functional (B3LYP),[21,22] that uses the correlation functional of Lee, Yang, and Parr,[23] in conjunction with Dunning's correlation-consistent cc-pVDZ basis set.[24] The same level of theory was used for frequency analysis to characterize local energy minima (all real frequencies) and transition structures (one imaginary frequency). Zero-point vibrational energy (ZPVE) and enthalpy corrections were calculated from B3LYP/cc-pVDZ harmonic frequencies. To obtain more accurate energies, in the second step we repeated the calculations using the G3B3 methodology[25] that combines the composite G3 theory[26] and B3LYP geometries and zero-point energies.

Results and Discussion

Direct Proton Transfer. Figure 1 shows the mass spectra obtained for the reaction of mass-selected $C_2H_5^+$ (m/z 29.0) with C_6H_6 recorded at nominal collision energies of 1.3 and 4.5 eV in the center-of-mass frame. As expected, the most intense channel is represented by proton transfer (PT) giving the products $C_6H_7^+$ and C_2H_4. Similar results have been obtained using deuterated benzene (Figure 2).

$$C_2H_5^+ + C_6H_{6-n}D_n \rightarrow C_6H_{7-n}D_n^+ + C_2H_4 \qquad (7a)$$

Assuming that the proton transfer according to reaction 7a leads to the formation of ethene concomitant with the most stable among the $C_6H_{7-n}D_n^+$ isomer ($n = 0, 6$), i.e., protonated benzene in the σ-complex structure,[27] the process is exothermic by 0.87 eV using literature values for the proton affinity of benzene, and by about 0.73 eV according to our calculations reported below.

The PT channel (reaction 7) has been studied by measuring the ratio I_P/I_0 (see the Experimental Methods section for definition and details) as a function of the benzene-d_6 density in the scattering cell. Results are shown in Figure 3 for the collision energy in the laboratory reference frame $E_{LAB} = 1.3$ eV (corresponding to ~1.0 eV in the center of mass frame). The data behave linear to density up to a value of about 2×10^{12} molecules·cm^{-3}. From the best fit, a value of 7 ± 2 Å^2 is derived for the absolute value of the proton-transfer cross section.

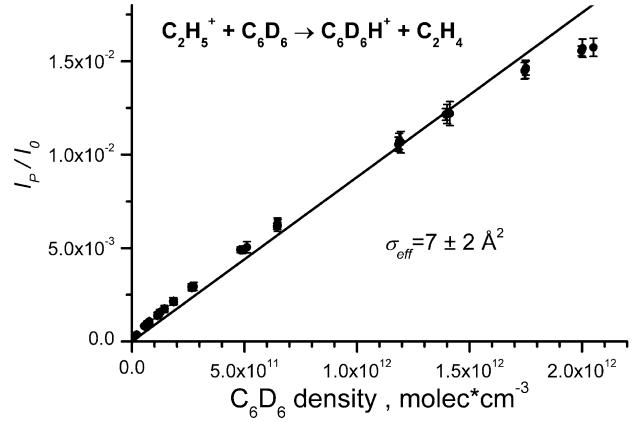

Figure 3. Density dependence of the $C_6D_6H^+$ product of the proton-transfer reaction from $C_2H_5^+$ to C_6D_6 at a collision energy $E_{LAB} = 1.3$ eV. The solid line is a linear fit of the data.

The negative deviation from linearity observed at higher densities in Figure 3, though not dramatic, might be attributed to the opening of other reactive channels, namely adduct formation affording $C_8H_5D_6^+$ products. The latter can efficiently compete with the proton-transfer channel at higher pressures due to collisional stabilization of the excited addition product (see discussion below).

Reactive integral cross sections for the proton transfer according to reaction 7 have further been measured as a function of the collision energy in the range 0.3−10 eV at a benzene pressure of ~3.0×10^{-6} mbar to ensure single collision conditions. In conjunction with the absolute cross section derived from Figure 3, the cross section as a function of the collision energy was derived (Figure 4). In the case of C_6H_6, the absolute value of the cross section was not measured and therefore data are shown in Figure 4 as cross sections in arbitrary units. We note that the collision energy dependences for benzene and its deuterated analogue are identical.

The cross section of reaction 7 shows a negative energy dependence, in agreement with a barrierless exothermic process.

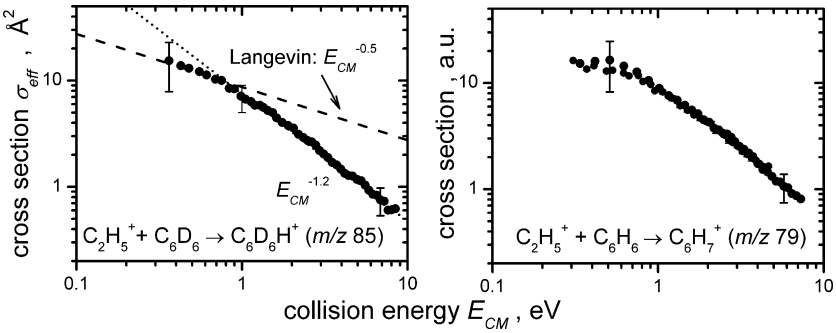

Figure 4. Cross section as a function of the collision energy for the reaction of $C_2H_5^+$ with C_6D_6 (left) and C_6H_6 (right) leading to the proton-transfer products $C_6D_6H^+$ and $C_6H_7^+$ respectively. Dashed and dotted lines in the left graph correspond to $E_{CM}^{-0.5}$ (Langevin model) and $E_{CM}^{-1.2}$ dependences, respectively (see text). The absolute value of the cross section has been measured directly, as described in the text, only in the case of benzene-d_6 and therefore the vertical scale in the right graph is given in arbitrary units.

In the low collision energy regime and up to about 0.8 eV, the cross section dependence on energy is qualitatively well reproduced by the Langevin model, predicting an $E_{CM}^{-0.5}$ behavior (dashed line in Figure 4). At energies >1 eV, the decrease of the cross section as the collision energy increases is more dramatic and it fits with a $E_{CM}^{-1.2}$ dependence (dotted line in Figure 4). Absolute cross section values can be converted into rate constants by using the expression for the phenomenological rate constant $k = \langle v \rangle \cdot \sigma$ where k is the rate constant in cm^3 s^{-1}, σ is the reaction cross section in cm^2 and $\langle v \rangle$ is the average relative velocity of reactants in cm·s^{-1}.[18] By applying this expression and using the experimental data measured at the lowest collision energies (i.e., $\sigma_{eff} = 15$ Å^2 at $E_{CM} = 0.4$ eV), we obtain a value of about 2.9×10^{-10} cm^3 s^{-1} for the rate constant of reaction 7.

C−C Coupling Reactions. Most interesting in Figures 1 and 2 is the observation of C−C bond forming reactions. In the case of benzene-h_6, the occurrence of such reactions is evidenced by signals due to the ions $C_8H_{11}^+$ (*m/z* 107), $C_7H_7^+$ (*m/z* 91), $C_8H_9^+$ (*m/z* 105), and $C_8H_7^+$ (*m/z* 103) in the mass spectrum recorded at low collision energy (see inset c) in Figure 1). In conjunction with the confirming mass shifts observed upon (Figure 2), the generation of these ions is attributed to the occurrence of reactions 9−12.

$$C_2H_5^+ + C_6H_6 \rightarrow C_8H_{11}^+ \text{ (}m/z\text{ 107)} \quad (9)$$

$$\rightarrow C_7H_7^+ \text{ (}m/z\text{ 91)} + CH_4 \quad (10)$$

$$\rightarrow C_8H_9^+ \text{ (}m/z\text{ 105)} + H_2 \quad (11)$$

$$\rightarrow C_8H_7^+ \text{ (}m/z\text{ 103)} + 2H_2 \quad (12)$$

To shed light on the mechanisms of the C−C coupling reactions 9−12, we have performed theoretical calculations of the most relevant stationary states of the $C_2H_5^+ + C_6H_6$ potential-energy surface (PES). Calculations have been carried out using two different levels of theory (B3LYP/cc-pVDZ and G3B3; see the section on Theoretical Methods). The optimized geometries of the minima and transition structures are shown in Figure 5. Table 1 summarizes the calculated results for energies and enthalpies of all relevant stationary points relative to the $C_2H_5^+ + C_6H_6$ reactant channel, while Scheme 1 shows a simplified energy diagram for the most relevant stationary states of the PES.

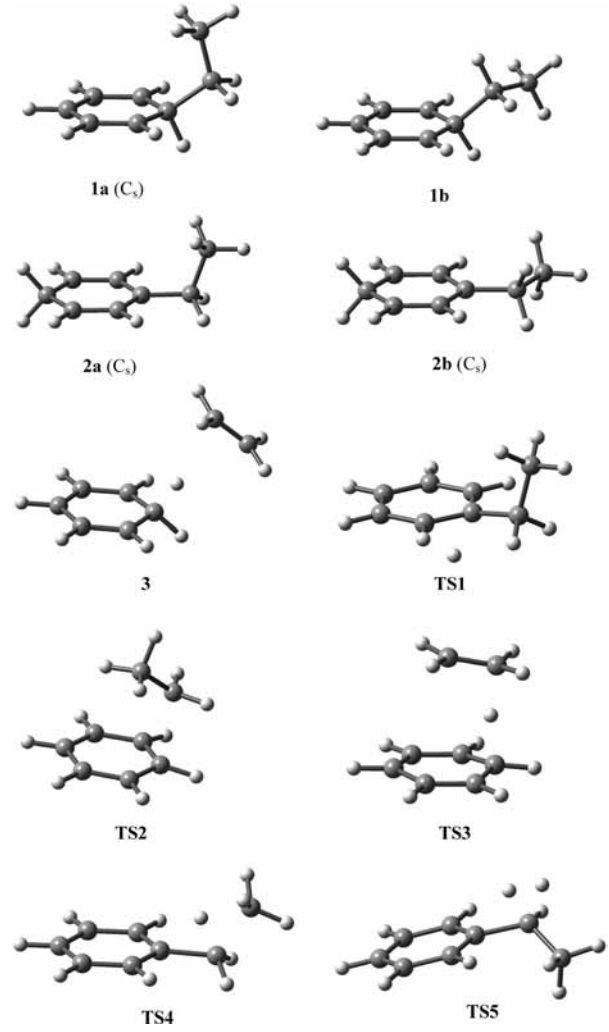

Figure 5. Structures of some minima and transition states of the $C_2H_5^+ + C_6H_6$ system optimized at the B3LYP/cc-pVDZ level of theory.

Among the isomers considered in this work, the most stable $C_8H_{11}^+$ cation results from the electrophilic addition of the ethyl cation $C_2H_5^+$ to the benzene ring to yield protonated ethylbenzene.[28] Such ion can carry the proton attached to any of the carbon atoms of the benzene ring, giving rise to four different isomers. For each tautomer, several minima on the PES can be found, corresponding to different conformers.

As already reported,[15a] the most stable tautomer corresponds to protonation at the para-position and stability of the other structures decreases according to the following order: para > ortho > meta >

TABLE 1: Calculated Energies and Enthalpies of the Relevant Minima, Transition Structures, and Dissociation Asymptotes[a] Relative to the $C_2H_5^+ + C_6H_6$ Channel[b]

	B3LYP/cc-pVDZ		G3B3	
ion/TS/reaction products	ΔE_{0K}	ΔH_{298K}	ΔE_{0K}	ΔH_{298K}
1a	–175	–177	–178	–180
1b	–175	–177	–175	–177
2a	–214	–215	–213	–214
2b	–214	–216	–211	–213
3	–102	–98	–90	–87
TS1	–153	–156	–161	–164
TS2	–118	–121	–130	–132
TS3	–83	–84	–77	–77
TS4	–29	–31	–33	–35
TS5	–28	–31	–38	–41
$C_2H_5^+ + C_6H_6$	0	0	0	0
$C_2H_4 + C_6H_7^+$	–82	–80	–69	–68
$C_7H_7^+$ (Bz^+)[c] $+ CH_4$	–167	–165	–156	–154
$C_7H_7^+$ (Tr^+)[c] $+ CH_4$	–204	–202	–185	–183
$C_6H_5CHCH_3^+ + H_2$	–165	–160	–155	–150
$C_6H_5^+ + C_2H_6$	53	55	61	63
$C_6H_5^+ + C_2H_4 + H_2$	187	197	187	197

[a] The labeling of the minima and transition structures refers to the optimized structures given in Figure 5. [b] The values are in kJ·mol^{-1} and are corrected for ZPVE. [c] Bz^+ and Tr^+ stand for the well-known benzylium and tropylium isomers of the $C_7H_7^+$ ion.

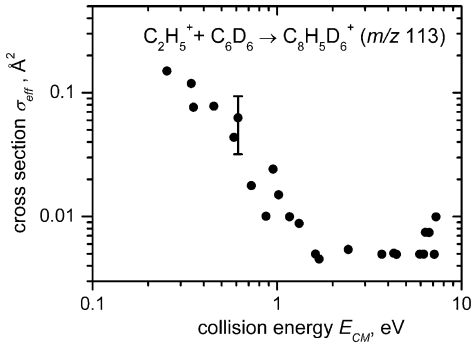

Figure 6. Cross section for the association of $C_2H_5^+$ with C_6D_6 to the product ion $C_8H_5D_6^+$ (*m/z* 113) as a function of the collision energy E_{CM}.

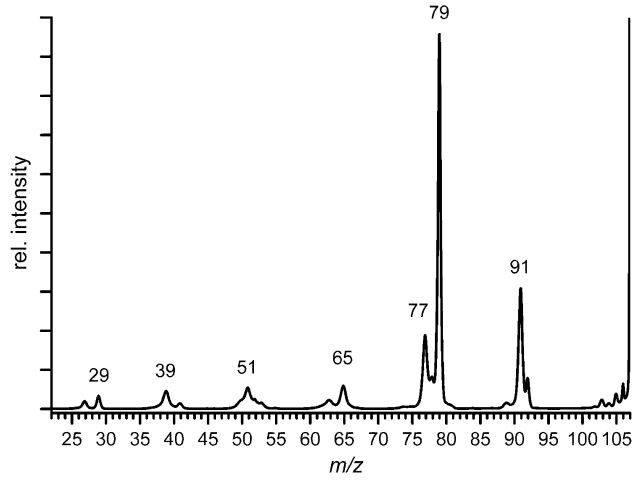

Figure 7. CID-MIKE spectrum of mass-selected $C_8H_{11}^+$ ions (*m/z* 107) produced by chemical ionization (CH_4) of ethylbenzene.

ipso, in accordance with the general trend of local proton affinities of the tautomeric protonated alkylbenzenes.[12,29]

These tautomers can easily interconvert into each other by a hydrogen "ring-walk".[12b–e,30,31] All the energy minima and associated transition structures relevant to these isomerization processes were calculated for the purposes of this study; however, a full description of the corresponding part of the PES is not reported here in details, as we believe it not to be relevant for the scope of this paper. Nevertheless, it is worth mentioning that ipso-protonated ethylbenzene (structure **1a**, see Figure 5) lies at −178 kJ mol^{-1} whereas the para-protonated tautomer (structure **2a**; see Figure 5) lies at −213 kJ mol^{-1} with respect to reagents (G3B3 level of theory and 0 K; see Table 1). Therefore, assuming para-protonated ethylbenzene as the final product of reaction 9, the latter is exoergic by 2.2 eV, which compares well to a value of 2.4 eV derived from the NIST data for the proton affinity of ethylbenzene.[32] None of the barriers associated with hydrogen ring-walk was found to exceed 60 kJ mol^{-1} relative to the energy of para-protonated ethylbenzene (at the G3B3 level, 0 K), indicating that equilibration of the ring protons is facile. For instance, H migration from the ipso position (structure **1a** in Scheme 1 and Figure 5) to the ortho position (structure not shown in Scheme 1 and Figure 5) occurs via the transition structure **TS1** that lies 161 kJ mol^{-1} below reagents, thus giving a barrier of 17 kJ mol^{-1}. Accordingly, protonated ethylbenzene is a highly dynamical system, in which all ring hydrogen atoms get scrambled once the internal energy exceeds approximately 60 kJ mol^{-1}. In addition to the hydrogen ring-walk, an ethyl cation migration around the benzene ring can also occur. The corresponding transition structure **TS2** lies at −130 kJ mol^{-1} (at the G3B3 level, 0 K), resulting in a barrier of 48 kJ mol^{-1} for ethyl migration from ipso-protonated ethylbenzene, i.e., only somewhat higher than the barriers associated with the hydrogen shifts along the ring.

Formation of the $C_8H_{11}^+$ ion is observed experimentally, though in rather low yield. Interestingly, its intensity strongly increases when the pressure in the scattering cell is increased above 10^{-4} mbar, indicating that multiple collisions allow efficient dissipation of the energy liberated upon association, thus providing stabilization of the initially excited addition product into a long-lived ion.[33] In the idealized gas phase, i.e., without occurrence of termolecular collisions, several other overall exothermic channels can compete (i.e., the losses of H_2, CH_4, and C_2H_4; Table 1) and thereby explain the low yield of reaction 9 in the collision experiment carried out in the multipole device.

The cross section of reaction 9 as a function of the collision energy, measured at sufficiently low pressure to avoid multiple collisions and using benzene-d_6 as neutral partner, is reported in Figure 6. The energy behavior is consistent with the formation of a long-lived addition complex, most likely the covalently bound protonated ethylbenzene. We note further that the probability for formation of the addition product is at least 2 orders of magnitude smaller than the proton-transfer channel (reaction 7) at the smallest collision energies available in our experimental setup.

The formation of a long-lived reaction complex between benzene and alkyl cations has been investigated in previous studies carried out at higher pressures.[6,8,10] In earlier studies of the reactions between $C_nH_{2n+1}^+$ and $C_nH_{2n-1}^+$ ions ($n = 2, 3$) and benzene in a pressure range of 10−20 μbar,[10] collisionally stabilized adduct products have been observed to compete with proton transfer to afford protonated benzene concomitant with elimination of an alkene molecule.

In the case of $C_3H_7^+$ ions, a unimolecular rate constant of 10^7 s^{-1} for the decomposition of the $C_9H_{13}^+$ adduct has been estimated and the authors predict that adduct formation should be the main channel for the reaction at pressures in excess of

SCHEME 1: Schematic Representation of the Most Relevant Stationary States of the $C_2H_5^+$ + Benzene System[a]

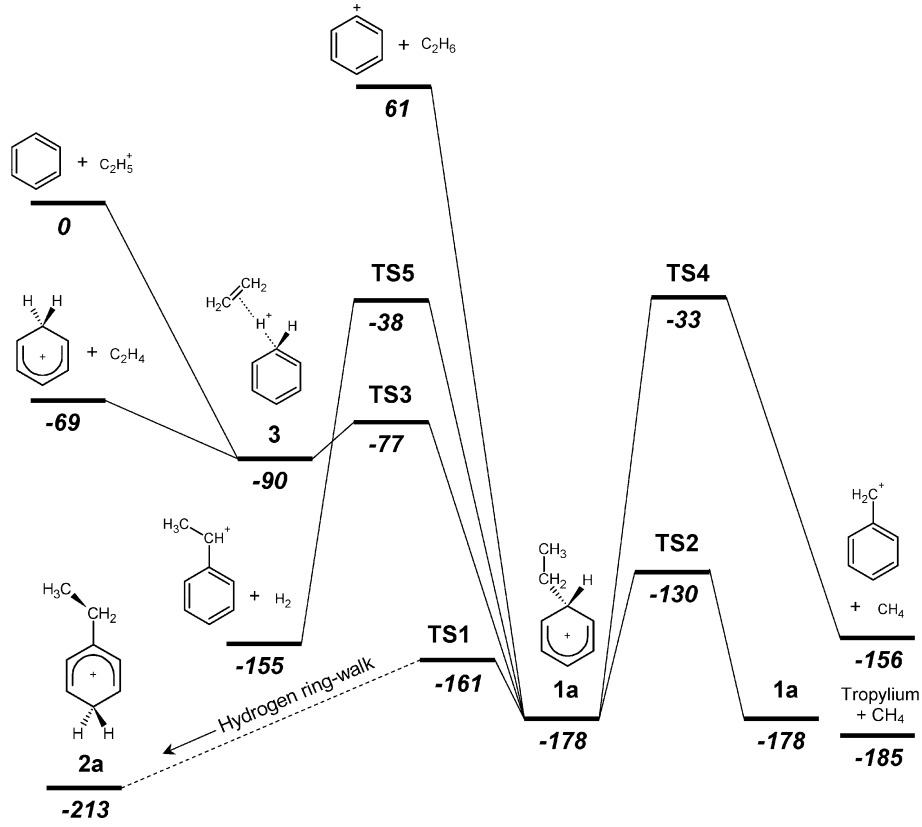

[a] The reported energy values (in kJ·mol^{-1}) are at the G3B3 level, 0 K. The labeling of minima and transition structures refers to Figure 5.

about 10 mbar. Further, by use of a combined radiolytic and mass spectrometric approach, the gas-phase ethylation of benzene has been shown to afford protonated ethylbenzene, and to proceed via a short-lived ion−neutral complex $C_6H_6\cdots C_2H_5^+$ whose lifetime was found to be 2×10^{-10} s at 298 K.[6] We point out that the transit time of the adduct through our instrument, in the CM collision energy range 0.2−1 eV shown in Figure 6, is of the order of 10−100 μs. Therefore, the $C_8H_5D_6^+$ ion observed cannot be the short-lived ion−neutral complex (e.g., structure 3 in Scheme 1), but the covalently bound protonated ethylbenzene into which the charged intermediate evolves. However, the association reaction 9, which is only a minor channel in our low-pressure experiments is suggested to occur as a major route at slightly elevated pressures. With respect to the atmosphere of Titan, having a surface pressure of about 1 bar and generally much lower temperatures, reaction 9 is thus very likely to occur and may even fully suppress proton transfer according to reaction 7. Accordingly, reaction 9 must be included as a significant seam for the growth of larger hydrocarbon ions via C−C coupling in the atmosphere of Titan. In turn, however, the computed PES also suggests that, once being formed, protonated ethylbenzene can undergo decomposition reactions to yield $C_6H_7^+ + C_2H_4$ or also $C_7H_7^+ + CH_4$ and $C_8H_9^+ + H_2$ (Scheme 1), and these processes thus represent possible sinks for the density of $C_8H_{11}^+$ ions in the atmosphere of Titan.

To shed further light on these putative fragmentation reactions, additional experiments with protonated ethylbenzene were performed. To this end, ethylbenzene was admitted to the chemical ionization source of a VG-ZAB2-SEQ tandem mass spectrometer which was fed with a large excess of methane as reagent gas. The so-formed $C_8H_{11}^+$ ion was mass-selected and subjected to a CID-MIKES experiment (Figure 7). The main fragmentation channels of protonated ethylbenzene are summarized in reactions 13−16.

$$C_8H_{11}^+ \ (m/z\ 107) \rightarrow C_6H_7^+ \ (m/z\ 79) + C_2H_4 \quad (13)$$

$$\rightarrow C_7H_7^+ \ (m/z\ 91) + CH_4 \quad (14)$$

$$\rightarrow C_6H_5^+ \ (m/z\ 77) + C_2H_4 + H_2 \quad (15)$$

$$\rightarrow C_8H_9^+ \ (m/z\ 105) + H_2 \quad (16)$$

The major fragmentation reactions observed in the CID-MIKE spectrum of protonated ethylbenzene lead to products that are also observed in the reaction of $C_2H_5^+$ with C_6H_6 carried out with the GIB setup. Accordingly, we conclude that the encounter complex produced in the reaction of ethyl cation with benzene can rearrange into protonated ethylbenzene and further dissociates into other channels. As amply shown by the fundamental works of Kuck on the mass spectrometry of alkylbenzenes[12] and in related experimental and theoretical studies,[1,14,15a,b,34] the main fragmentation channel of ethylbenzenium ions is the elimination of an ethylene molecule leading to $C_6H_7^+$. The overall process $C_2H_5^+ + C_6H_6 \rightarrow C_8H_{11}^+ \rightarrow C_6H_7^+ + C_2H_4$ is mass-spectrometrically indistinguishable from the direct proton-transfer channel (7) described above. The fact that the cross section for m/z 79 (and 85 when using C_6D_6) shown in Figure 4 steeply decreases with E_{CM}, indicates a preference of proton transfer via complex formation rather than its occurrence as a direct proton transfer. Nevertheless, the reaction is quasi-irreversible because no sign for the occurrence of H/D exchange of the $C_2H_5^+$ reactant ion (e.g., $C_2H_4D^+$, m/z 30) is observed in

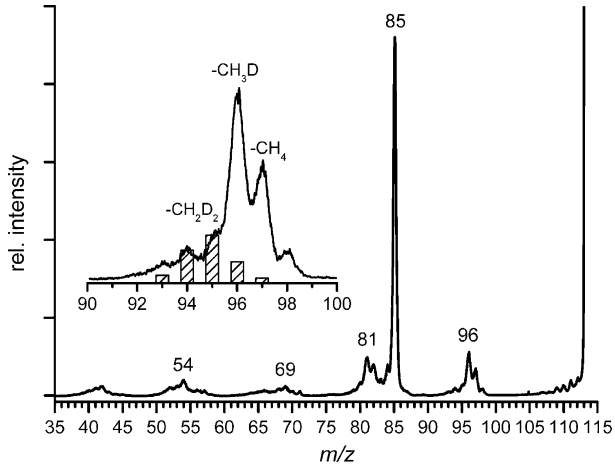

Figure 8. CID-MIKE spectrum of $C_8D_6H_5^+$ ions (*m/z* 113) produced by chemical ionization of a mixture of C_6D_6 and C_2H_5OH registered with a ZAB instrument. The inset shows an expanded view of the methane-loss region. The hatched bars give the expected statistical pattern for methane elimination (normalized to the observed intensity of the CH_2D_2 loss channel). The presence of a peak at *m/z* 98 could correspond not only to a CH_3 loss but also to the loss of $^{12}CH_3$ from isobaric ions $^{13}C^{12}C_7D_6H_4^+$ having the structure of ethylbenzene cation which is known to lose a methyl radical.[35,39]

the reaction with C_6D_6 (Figure 2a). Likewise, the weak signal observed at *m/z* 84 in Figure 2a is assigned to the incompleteness of the deuterium label in the sample (99.5 atom % D, and thus ca. 3% C_6HD_5), rather than H/D exchange.

The second most abundant fragmentation channel in the CID-MIKE spectrum of ethylbenzenium ions corresponds to the loss of CH_4 to give a $C_7H_7^+$ ion. The production of a $C_7H_7^+$ ion is observed also as a product of the reaction of ethyl cation with benzene, although in much smaller yield than the proton-transfer product $C_6H_7^+$. The methane elimination channel in the CID-MIKE spectrum of protonated ethylbenzene has been also studied using partial D-labeling from the ion $C_8D_6H_5^+$ (*m/z* 113) produced from chemical ionization of a mixture of C_6D_6 and C_2H_5OH. The corresponding CID-MIKE spectrum (Figure 8) exhibits predominant losses of CH_3D and CH_4 and only minor contributions of CH_2D_2, CHD_3, and CD_4 (i.e., CH_4:CH_3D:CH_2D_2:CHD_3:CD_4 = 27:44:12:10:7, when normalized to Σ = 100). Extensive H/D equilibration is thus evident, although the distribution still shows a preference for the inclusion of the H-atoms stemming from ethanol used as reagent, as demonstrated by the significant deviation from the expected statistical pattern for $C_8H_5D_6^+$ (i.e., CH_4:CH_3D:CH_2D_2:CHD_3:CD_4 = 5:30:45:18:2; given as hatched columns in Figure 8). It is in fact well-known that the lowest energy isomer of $C_7H_7^+$ ions is the tropylium ion (Tr^+), while the benzylium structure (Bz^+) lies about 0.71 eV higher in energy.[35] When starting from ethyl cation plus benzene, the overall reaction 10 is exothermic by 2.10 eV for Tr^+ formation and by 1.54 eV if Bz^+ is produced,[36] which is in good agreement with our calculated values of 1.92 and 1.62 eV at the G3B3 level. However, although the barrier calculated for methane elimination concomitant with formation of the Bz^+ isomer via the transition state **TS4** lies below the $C_2H_5^+ + C_6H_6$ entrance channel, it is too high to account for the observed pronounced competition of CH_4 and C_2H_4 losses shown in Figure 7. Most likely, an intimate rearrangement to the more stable tropylium ion is involved in the fragmentation process,[37] which we have not studied further in this context. Alternatively, fragmentation with methane loss might involve ring expansion to methyldihydrotropylium ion and contraction to protonated xylenes, as reported in detail in ref 38. In fact, when starting from the partially labeled $C_8D_6H_5^+$ ions (assuming a structure in which the five H atoms are on the ethyl group, while the six D atoms are on the aromatic ring), the mechanistic path **1a** → **TS4** → $Bz^+ + CH_4$ would lead exclusively to the loss of CH_3D and therefore would not explain the other fragments observed in the region of the methane losses (Figure 8). Conversely, expansion to the seven-ring member opens up the pathway for H/D exchange between the methyl and ring hydrogen atoms and might explain the degree of H scrambling observed in the methane loss channel.[13,14a,38]

As far as the minor product ions in the MIKE spectra are concerned, these agree with the results of the GIB experiments, i.e., molecular hydrogen losses to give ions $C_8H_9^+$, *m/z* 105, and $C_8H_7^+$, *m/z* 103, as a consecutive product (see Figure 1), or can be ascribed to well-known consecutive fragmentations in the mass spectrometry of aromatic ions, e.g., $C_6H_7^+ \rightarrow C_6H_5^+ \rightarrow C_4H_3^+$ and $C_7H_7^+ \rightarrow C_5H_5^+$, and will thus not be detailed any further.

Conclusions

By combined experimental and theoretical work, we have reinvestigated the reaction of ethyl cation with benzene with particular attention to its possible relevance for chemical processes in the atmosphere of Saturn's moon Titan. Consistent with earlier reports, we observed proton transfer to afford $C_6H_7^+$ (i.e., protonated benzene) as the major channel under the idealized conditions of strictly bimolecular collisions. Further, the reactive cross section of the proton-transfer process has been determined for the first time. The energy behavior of the cross section indicates that the reaction, though quasi-irreversible, proceeds via the formation of covalently bound adducts, such as the para-protonated ethylbenzene as the most stable isomer. This conjecture is supported by the observation of several other channels, albeit with much smaller intensities, which confirm the occurrence of C−C coupling processes in the reaction of $C_2H_5^+$ with benzene. The analysis of the experimental and theoretical results in fact implies that under the conditions of Titan's atmosphere, termolecular association of $C_2H_5^+$ with benzene to afford protonated ethylbenzene is very likely to occur. In a more general context, the condensation of alkyl cations with preformed neutral arenes thus provides a new route for the growth of larger hydrocarbon molecules in the atmospheres of methane-rich planets or moons.

Acknowledgment. We thank Zdenek Herman for helpful discussions. This work was supported by the bilateral scientific cooperation agreement AVCR-CNR 2007-09 of the Academy of Sciences of the Czech Republic and the Italian Consiglio Nazionale delle Ricerche. Additional funding was provided by the Academy of Sciences of the Czech Republic (Z40550506), the Grant Agency of the Academy of Sciences of the Czech Republic (IAA400400702), the Grant Agency of the Czech Republic (203/09/1223), the Ministry of Education of the Czech Republic (MSM0021620857, RP MSMT 14/63), the EPSRC (EP/E038522/1) and the University of Trento. J.R. acknowledges support of her research on the chemistry of Titan by a L'Oreal "For Women in Science" stipend.

References and Notes

(1) (a) Waite, J. H., Jr.; Niemann, H.; Yelle, R. V.; Kasprzak, W. T.; Cravens, T. E.; Luhmann, J. G.; Mcnutt, R. L.; Ip, W.-H.; Gell, D.; De La Haye, V.; Müller-Wordag, I.; Magee, B.; Borggren, N.; Ledvina, S.; Fletcher, G.; Walter, E.; Miller, R.; Scherer, S.; Thorpe, R.; Xu, J.; Block, B.; Arnett, K. *Science* **2005**, *308*, 982. (b) Waite, J. H., Jr.; Young, D. T.; Cravens, T. E.; Coates, A. J.; Cray, F. J.; Magee, B.; Westlake, J. *Science* **2007**, *316*, 870.

(2) Keller, C.; Anicich, V.; Cravens, T. *Planet. Space Sci.* **1998**, *46*, 1157–1174.

(3) Anicich, V. G.; Wilson, P. F.; McEwan, M. J. *J. Am. Soc. Mass Spectrom.* **2006**, *17*, 544.

(4) Ricketts, C. L.; Schröder, D.; Alcaraz, C.; Roithová, J. *Chem.—Eur. J.* **2008**, *14*, 4779.

(5) (a) Anicich, V. G. *An Index of the Literature for Bimolecular Gas Phase Cation-Molecule Reaction Kinetics*; JPL Publication 03-19; Jet Propulsion Laboratory: Pasadena CA, 2003. (b) McEwan, M. J.; Anicich, V. G. *Mass Spectrom. Rev.* **2007**, *26*, 281.

(6) Aschi, M.; Attina, M.; Cacace, F. *Chem.—Eur. J.* **1998**, *4*, 1535–1541.

(7) (a) Vuitton, V.; Yelle, R. V.; Anicich, V. G. *Astrophs. J.* **2006**, *647*, L175. (b) Vuitton, V.; Yelle, R. V.; McEwan, M. J. *Icarus* **2007**, *191*, 722.

(8) Audier, H. E.; Monteiro, C.; Robin, D. *New J. Chem.* **1989**, *13*, 621.

(9) Tanaka, Y.; Tsuji, M. *Bull. Chem. Soc. Jpn.* **2002**, *75*, 241.

(10) Bone, L. I.; Futrell, J. H. *J. Chem. Phys.* **1967**, *47*, 4366.

(11) Morrison, J. D.; Stanney, K.; Tedder, J. M. *J. Chem. Soc. Perkin 2* **1981**, 838.

(12) (a) Kuck, D. *Mass Spectrom. Rev.* **1990**, *9*, 187. (b) Kuck, D. *Mass Spectrom. Rev.* **1990**, *9*, 583. (c) Kuck, D. *Int. J. Mass Spectrom.* **2002**, *213*, 101. (d) Kuck, D. Protonated Aromatics and Arenium Ions. In *Encyclopedia of Mass Spectrometry*; Nibbering, N. M. M., Ed.; Elsevier: Amsterdam, 2005; Vol. 4, Topic B16, p 229. (e) Kuck, D. H/D Exchange in Hydrocarbon Ions. In *Encyclopedia of Mass Spectrometry*; Nibbering, N. M. M., Ed.; Elsevier: Amsterdam, 2005; Vol. 4, Topic B20, p 270.

(13) (a) Mormann, M.; Kuck, D. *Int. J. Mass Spectrom.* **2001**, *210/211*, 531. (b) Mormann, M.; Kuck, D. *Int. J. Mass Spectrom.* **2002**, *219*, 497. (c) Mormann, M.; Decker, B.; Kuck, D. *Int. J. Mass Spectrom.* **2007**, *267*, 148. (d) Sekiguchi, O.; Meyer, V.; Letzel, M. C.; Kuck, D.; Uggerud, E. *Eur. J. Mass Spectrom.* **2009**, *15*, 167.

(14) (a) Arstad, B.; Kolboe, S.; Swang, O. *J. Phys. Org. Chem.* **2004**, *17*, 1023. (b) Arstad, B.; Kolboe, S.; Swang, O. *J. Phys. Org. Chem.* **2006**, *19*, 81.

(15) (a) Kolboe, S.; Svelle, S.; Arstad, B. *J. Phys. Chem. A* **2009**, *113*, 917. Addition/correction. *J. Phys. Chem. A* **2009**, *113*, 1869. (b) Sancho-Garcia, J. C. *Chem. Phys. Lett.* **2009**, *468*, 138. (c) van Mourik, T. *J. Phys. Chem. A* **2008**, *112*, 11017. (d) Kolboe, S.; Svelle, S. *J. Phys. Chem. A* **2008**, *112*, 6399.

(16) Andrei, H.-S.; Solcà, N.; Dopfer, O. *Angew. Chem., Int. Ed.* **2008**, *47*, 395.

(17) (a) Bassi, D.; Tosi, P.; Schlogl, R. *J. Vacuum Science Technol. A-Vacuum Surf. Films* **1998**, *16*, 114. (b) Ascenzi, D.; Cont, N.; Guella, G.; Franceschi, P.; Tosi, P. *J. Phys. Chem. A* **2007**, *111*, 12513. (c) Franceschi, P.; Penasa, L.; Ascenzi, D.; Bassi, D.; Scotoni, M.; Tosi, P. *Int. J. Mass Spectrom.* **2007**, *265*, 224.

(18) Ervin, K. M.; Armentrout, P. *J. Chem. Phys.* **1985**, *83*, 166.

(19) (a) Roithová, J.; Schröder, D. *Phys. Chem. Chem. Phys.* **2007**, *9*, 731. (b) Roithová, J.; Schröder, D.; Míšek, J.; Stará, I. G.; Starý, I. *J. Mass Spectrom.* **2007**, *42*, 1233.

(20) Frisch, M. J.; Trucks, G. W.; Schlegel, H. B.; Scuseria, G. E.; Robb, M. A.; Cheeseman, J. R.; Montgomery, J. A., Jr.; Vreven, T.; Kudin, K. N.; Burant, J. C.; Millam, J. M.; Iyengar, S. S.; Tomasi, J.; Barone, V.; Mennucci, B.; Cossi, M.; Scalmani, G.; Rega, N.; Petersson, G. A.; Nakatsuji, H.; Hada, M.; Ehara, M.; Toyota, K.; Fukuda, R.; Hasegawa, J.; Ishida, M.; Nakajima, T.; Honda, Y.; Kitao, O.; Nakai, H.; Klene, M.; Li, X.; Knox, J. E.; Hratchian, H. P.; Cross, J. B.; Bakken, V.; Adamo, C.; Jaramillo, J.; Gomperts, R.; Stratmann, R. E.; Yazyev, O.; Austin, A. J.; Cammi, R.; Pomelli, C.; Ochterski, J. W.; Ayala, P. Y.; Morokuma, K.; Voth, G. A.; Salvador, P.; Dannenberg, J. J.; Zakrzewski, V. G.; Dapprich, S.; Daniels, A. D.; Strain, M. C.; Farkas, O.; Malick, D. K.; Rabuck, A. D.; Raghavachari, K.; Foresman, J. B.; Ortiz, J. V.; Cui, Q.; Baboul, A. G.; Clifford, S.; Cioslowski, J.; Stefanov, B. B.; Liu, G.; Liashenko, A.; Piskorz, P.; Komaromi, I.; Martin, R. L.; Fox, D. J.; Keith, T.; Al-Laham, M. A.; Peng, C. Y.; Nanayakkara, A.; Challacombe, M.; Gill, P. M. W.; Johnson, B.; Chen, W.; Wong, M. W.; Gonzalez, C.; and Pople, J. A. *Gaussian 03*, revision C.02; Gaussian, Inc.: Wallingford, CT, 2004.

(21) Becke, A. D. *J. Chem. Phys.* **1993**, *98*, 1372.

(22) Becke, A. D. *J. Chem. Phys.* **1993**, *98*, 5648.

(23) Lee, C.; Yang, W.; Parr, R. G. *Phys. Rev. B* **1988**, *37*, 785.

(24) Dunning, T. H., Jr. *J. Chem. Phys.* **1989**, *90*, 1007.

(25) Baboul, A. G.; Curtiss, L. A.; Redfern, P. C.; Raghavachari, K. *J. Chem. Phys.* **1999**, *110*, 7650.

(26) Curtiss, L. A.; Raghavachari, K.; Redfern, P. C.; Rassolov, V.; Pople, J. A. *J. Chem. Phys.* **1998**, *109*, 7764.

(27) Schröder, D.; Loos, J.; Schwarz, H.; Thissen, R.; Dutuit, O. *J. Phys. Chem. A* **2004**, *108*, 9931.

(28) Protonated xylenes are predicted to be even more stable isomers, see ref 13d.

(29) For combined spectroscopic/theoretical studies of the closely related case of protonated toluene, see: (a) Dopfer, O.; Lemaire, J.; Maitre, P.; Chiavarino, B.; Crestoni, M. E.; Fornarini, S. *Int. J. Mass Spectrom.* **2006**, *249*, 149. (b) Schröder, D.; Schwarz, H.; Milko, P.; Roithová, J. *J. Phys. Chem. A* **2006**, *110*, 8346. (c) Douberly, G. E.; Ricks, A. M.; Schleyer, P. v. R.; Duncan, M. A. *J. Phys. Chem. A* **2008**, *112*, 4869.

(30) Kuck, D. *Angew. Chem., Int. Ed.* **2000**, *39*, 125; *Angew. Chem.* **2000**, *112*, 129.

(31) Ascenzi, D.; Bassi, D.; Franceschi, P.; Hadjar, O.; Tosi, P.; Di Stefano, M.; Rosi, M.; Sgamellotti, A. *J. Chem. Phys.* **2004**, *121*, 6728.

(32) The value 788.0 $kJ \cdot mol^{-1}$ is taken for the proton affinity of ethylbenzene. Hunter, E. P. Lias, S. G. Proton Affinity Evaluation. In *NIST Chemistry Webbook*; NIST Standard Reference Database Number 69; Linstrom, P. J., Mallard, W. G., Eds.; National Institute of Standards and Technology: Gaithersburg, MD, 20899, http://webbook.nist.gov (retrieved June 30, 2009).

(33) Note, however, that a multipole setup is not ideally suited to study the pressure dependence of consecutive reactions and we therefore refrain from the explicit documentation of the data. For a discussion, see: Jagoda-Cwiklik, B.; Jungwirth, P.; Rulíšek, L.; Milko, P.; Roithová, J.; Lemaire, J.; Maitre, P.; Ortega, J. M.; Schröder, D. *ChemPhysChem* **2007**, *8*, 1629.

(34) Kameyama, S.; Inomata, S.; Tanimoto, H. *Int. J. Mass Spectrom.* **2008**, *276*, 49.

(35) Malow, M.; Penno, M.; Weitzel, K.-M. *J. Phys. Chem.* **2003**, *107*, 10625. (b) Fridgen, T. D.; Troe, J.; Viggiano, A. A.; Midey, A. J.; Williams, S.; McMahon, T. B. *J. Phys. Chem. A* **2004**, *108*, 5600.

(36) Derived from NIST thermodynamical data and the most accurate values for $\Delta_f H°(0K)$ of Tr^+ and Bz^+ as suggested in ref 35. NIST Standard Reference Database Number 69, Gaithersburg, 2008, see: http://webbook.nist.gov/chemistry/.

(37) (a) Zins, E.-L.; Pepe, C.; Rondeau, D.; Rochut, S.; Galland, N.; Tabet, J.-C. *J. Mass Spectrom.* **2009**, *44*, 12. (b) Zins, E.-L.; Pepe, C.; Schröder, D. *Faraday Discuss.* **2009**, in press.

(38) Mormann, M.; Kuck, D. *J. Mass Spectrom.* **1999**, *34*, 384.

(39) Schulze, S.; Paul, A.; Weitzel, K.-M. *Int. J. Mass Spectrom.* **2006**, *252*, 189.

JP905052H